In-situ sampling of lipids in tissues using a porous membrane microprobe for direct mass spectrometry analysis

Bin Jiao, Wei Zhou, Yikun Liu, Wenpeng Zhang [*], Zheng Ouyang [**]

State Key Laboratory of Precision Measurement Technology and Instruments, Department of Precision Instrument, Tsinghua University, Beijing, 100084, China

ARTICLE INFO

ABSTRACT

Direct sampling of lipids from tissues for direct mass spectrometry (MS) analysis allows a quick profiling of lipidome, which is important for biomedical applications. In this work, we developed a polyporous polymeric membrane (PPM) microprobe for highly efficient sampling of lipids directly from tissue samples. The PPM was prepared by polypropylene with pores as large of 10 μm, facilitating the permeation of lipids from tissue surfaces. The PPM was coated onto a stainless steel wire with a thickness of ~100 μm. The entire analysis procedure includes sampling of the lipids in tissue, washing the probe, and extraction spray ionization for MS analysis. The effectiveness was validated by analyzing mouse brain tissue samples. It showed high recoveries for a series of lipid classes in comparison with total lipid extraction method. Further demonstration was carried out with analysis of tissue samples from mouse liver, stomach, kidney and legs. With high physical strength and good chemical stability, the microprobe was also demonstrated for sampling lipids inside mouse kidney tissue samples. By incorporating a photochemical derivatization, a workflow was also developed for fast detection of lipid C═C isomers in tissue samples. Finally, a microprobe array was also developed for simultaneous sampling of lipids from multiple sites on tissue surfaces.

1. Introduction

Lipids play a crucial role in cell membrane formation [1,2], energy production and storage [3] as well as signal transduction [4,5]. The analysis of lipids can reveal ongoing biochemical processes in the organism and facilitate the biomarker discovery for disease diagnosis [6–10]. With the unique capability of structure identification and quantitation in mixtures, mass spectrometry (MS) has become a powerful tool for larger-scale profiling of lipids in biological systems and discovery of new lipid biomarkers [11–13]. With the developments in tandem MS methods involving new dissociation techniques [14–16] or coupling with chemical derivatizations [17,18], identification of detailed structures of lipids, such as C═C location and chain *sn*-positions, was also achieved using MS. This opens a new dimension for investigation of the function of lipid isomers [9,10,19,20].

Profiling of lipids in tissue samples usually requires extraction of lipids prior to analysis by MS. Total lipid extraction methods, such as Folch method [21], Bligh and Dyer method [22] and Soxhlet method [23], are widely used since they can efficiently transfer the lipids from tissue or biofluid samples into solvents for MS analysis. However, these

methods are usually complicated in operation and time-consuming. Development of tissue sampling probes is possible to facilitate direct MS analysis of lipids in tissue samples. Solid-phase microextraction (SPME) probes based on adsorbent coated fibers have been used for extraction of fatty acids in plasma samples [24]. Recently, our group also developed a transfer enrichment method based on porous polymer coating capillary for the fast sampling of fatty acids in blood samples [25].

Relatively less effort has been put in direct sampling of lipids from tissue samples. For the sampling of tissue samples, the probe needs to be mechanically durable and chemically stable [26,27], while possessing good adsorption efficiency towards target compounds. In this work, we developed a polyporous polymeric membrane (PPM) microprobe for highly efficient sampling of lipids directly from tissue samples. The PPM was prepared by polypropylene which possessed good chemical resistance and high mechanical strength [28–30] for direct sampling in hard tissue samples such as leg musculature. The PPM has abundant micropores, facilitating the permeation of lipids from tissue surfaces. After sampling, the PPM microprobe was used for MS analysis using extraction ionization [31–33], which enabled direct profiling of lipids within a

couple of minutes. Comparing with direct MS approaches such as ambient ionization-MS methods [34–37], the matrix effect would be significant reduced with the microsampling-based MS method, thus improving the sensitivity for the detection of different classes of lipids. The effectiveness of the microprobe has been validated by analysis of different kinds of mouse tissue samples. A microprobe array was also fabricated for simultaneous sampling at multiple sites, which would be useful to resolve the issue of heterogeneous distribution of lipids by small-scale tissue sampling techniques. Finally, by incorporating an online photochemical derivatization step, we also demonstrated the capability of the PPM microprobe method for fast profiling of lipid isomer biomarkers in tissue samples.

2. Experimental

2.1. Chemicals and materials

Dopamine hydrochloride was purchased from Sigma-Aldrich Corporation (St. Louis, Missouri, USA). Polypropylene, myristic acid, cysteine and diphenyl carbonate were purchased from Aladdin (Shanghai, China). Lipid standards were purchased from Avanti Polar Lipids, Inc. (Alabaster, AL, USA). HPLC grade solvents (ethyl acetate, acetonitrile, methanol and water) were purchased from Fisher Scientific (NJ, USA). Mice were supplied by the School of Life Sciences, Tsinghua University. Whole brain, stomach, leg and liver tissues were collected and stored at -80 $^\circ$C before use. The animal experiments were compliant with the ethical guidelines of the Tsinghua University Institutional Animal Care and Use Committee. Human breast cancer tissue samples were supplied by the specimen bank of Dongfeng Hospital of Hubei University of Medicine. All the procedures related to these samples were compliant with all relevant ethical regulations set by the Ethical Review Board of Tsinghua University.

2.2. Instrumentation

Scanning electron microscope (SEM) images were performed using a Nova NanoSEM™ scanning electron microscope (FEI Technologies Inc., Oregon, USA). Infrared spectroscopy (IR) spectra were collected using a VERTEX 70v FT-IR Spectrometer (Bruker Daltonics, Bremen, Germany). Mass spectrometry data were collected on a QTRAP 4500 mass spectrometer (SCIEX, Toronto, Canada) which possesses functions of neutral loss scan (NLS) and precursor ion scan (PIS), for direct profiling of different classes of lipids, and a TIMS-TOF mass spectrometer (Bruker Daltonics, Bremen, Germany) for the analysis of accurate mass of lipids extracted from the tissue samples based MS1 scan. LC-MS analyses were conducted on a Shimadzu LC-20AD system (Kyoto, Japan).

2.3. Preparation of the PPM microprobe

The polypropylene (PP) membranes were prepared from PP-binary diluent systems via thermally induced phase separation (TIPS) method. The binary diluent consisted of myristic acid and diphenyl carbonate. PP, myristic acid, and diphenyl carbonate powder with certain concentrations (weight ratio 2: 2: 3) were melt-blended in a three-necked flask at an elevated temperature (150 $^\circ$C) to obtain a homogenous dope solution. Subsequently, the solution was drawn with a plastic tip dropper and dropped onto a stainless steel wire (o.d. 300 μm or 600 μm) rotating at about 1000 rpm. Then the dope solution was immersed into a water bath at 50 $^\circ$C to induce phase separation. The diluent in the membrane was extracted by ethanol and the PP polyporous membrane was obtained after the volatilization of ethanol.

2.4. Hydrophilic modification

The membrane modification was carried out in two steps by poly-dopamine (PDA) coating and high temperature Michael addition reaction

[38–40]. For thin-layer coating of PDA, PP membranes were immersed in 20 mL of 10 mM Tris buffer solution (pH 8.5) containing 2 mg/mL dopamine hydrochloride at room temperature. The PDA-coated membranes were taken out and washed thoroughly with deionized water to remove loosely bound PDA. The cleaned membranes were dried under 25 $^\circ$C and the PDA-coated membranes were then functionalized with L-cysteine by performing a Michael addition reaction at 50 $^\circ$C. PDA-coated membranes were immersed into a flask containing 25 mL of 1 mg/mL L-cysteine solution in deionized water. The reaction was carried out for 12 h at 50 $^\circ$C. The obtained membranes were rinsed with deionized water for further use.

2.5. Sampling of lipids in tissue samples

The probe was fixed onto a 3D-printed cartridge, which consisted of a handle part and a substrate. For sampling of lipids from tissue samples, frozen tissue samples were thawed to room temperature. The probe was applied onto the tissue sample by means of rolling on the surface or inserting into the tissue. After sampling, the probe was dipped into a water solution for washing and finally inserting into a borosilicate glass capillary (1.5 mm o. d. and 0.86 mm i. d.) for elution and nanoESI-MS analysis.

3. Results and discussion

3.1. Preparation of the PPM microprobe for lipid sampling

In this work, we aimed at development of a microprobe for *in situ* sampling of lipids from tissue samples. Different from most commonly used liquid-liquid extraction methods [23,41], the proposed strategy allows for *in situ* sampling of lipids directly from the surface or the interior of a tissue sample. To avoid damage of the surface coating materials during sampling and other processes, a monolithic polymer membrane was selected for sampling of tissue samples. Polypropylene is mechanically rugged, chemically resistant to most organic solvents, and also has good biocompatibility, making it a good material candidate for sampling of tissue samples. As shown in Fig. 1, the stainless steel wire (~80 mm long and 600 μm in diameter) was coated by a microporous PP membrane with a thickness of ~100 μm. This design is to improve the sampling efficiency and facilitate the integration of sampling process with the following detection procedures. In a typical process, the probe was applied onto the surface of a tissue sample, lipid components in the tissue microenvironment would flow into the pores of the hollow PP membrane. After sampling, the probe can be coupled with nanoESI for fast and direct MS analysis.

The PPM was fabricated according to the procedure described in Fig. 2. Mixtures of PP, myristic acid and diphenyl carbonate (2: 2: 3, w/w/w) were heated to 150 $^\circ$C to obtain a homogenous solution. For the coating of PP, 10 μL of the hot solution was dropped onto the end of a stainless steel wire (300 μm o. d. or 600 μm o. d.) with a rotating speed of 1000 rpm. The PP-coated wire was then washed by ethanol to remove the
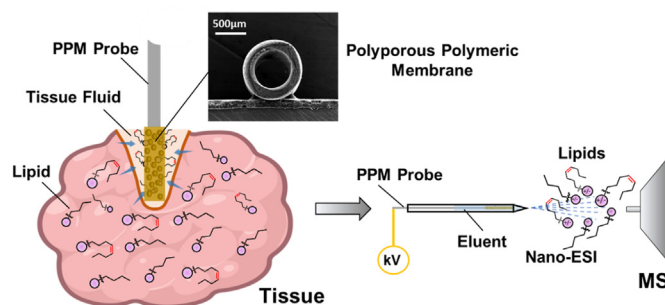

Fig. 1. Schematic diagram of the use of the microprobe for rapid sampling of biological tissues.
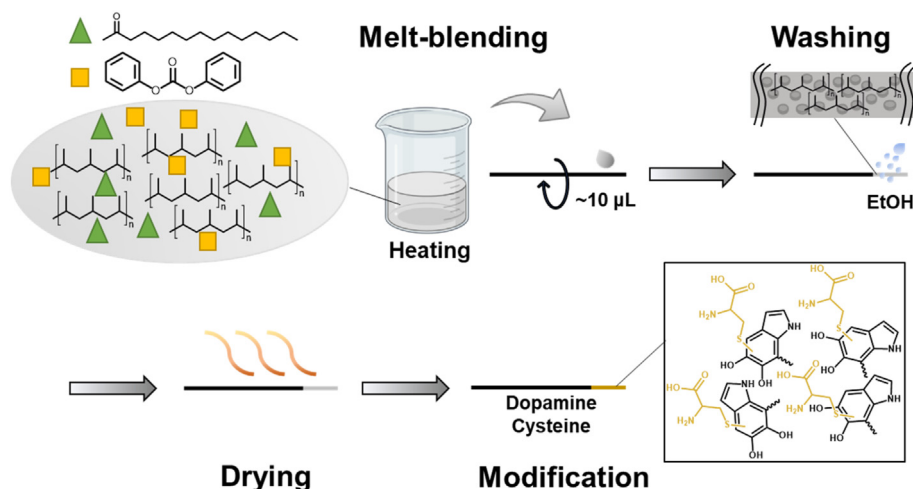
Fig. 2. Schematic of preparation of sampling microprobe, mainly including coating and modification on stainless steel wire.

porogen. Using polydopamine method, the PP membrane can be further modified with hydrophilic groups.

The morphology of the microprobe was characterized by SEM. As shown in Fig. 3 and Fig. S1, abundant pores were observed on the PPM, with diameters distributed between 5 and 20 μm. The outside of the skeleton of the PPM was relatively smooth, making it less destructive to tissue samples, and less possible to damage the polymer surface during interacting with hard tissues. Besides, the inner wall of channels consists of rough particles and many micropores, facilitating adsorption of lipids from tissue samples. The thickness of the PPM was adjusted by depositing different amounts of raw PP materials to the stainless-steel wire. The sampling efficiency of PPM with different thickness (10–200 μm) were compared for the sampling of PCs from mouse brain tissue samples. As shown in Fig. S4d, more PCs were obtained with the increase of the thickness of the PPM. However, thicker membrane would make it difficult to couple the microprobe with the nanoESI. Therefore, PPM with the thickness ~100 μm was used in consideration of both sampling efficiency and feasibility in analytical applications. Using myristic acid and diphenyl carbonate as the porogen, abundant pores at the scale of micrometers were obtained. To investigate the effect of the pore size,

different PPM were prepared by using single porogen (myristic or diphenyl carbonate) and mixed porogens (myristic:diphenyl carbonate, 2/3, w/w). Through evaluation by mouse brain tissue samples, PPM with mixed porogens showed higher sampling efficiency (Fig. S4e) than that with single porogen towards phospholipids. This is probably due to the better permeability of lipids by PPM with larger pores generated by mixed porogens.

The prepared PPM is strongly hydrophobic, with the water contact angle of 90° (Fig. 3e), which is helpful to hydrophobic interactions for sampling of non-polar compounds. However, the strong hydrophobicity of the surface could interfere the permeation of biological samples to the PPM. To improve of the wetting property of the PPM surface, it was further modified by a thin layer of PDA-cysteine. As shown in Fig. 3e, with in-solution PDA modification, the water contact angle was observed to decrease from 90° to 64° due to the incorporation of amine and phenol groups onto the surface of PPM. Through further modification of cysteine onto the PDA layer, the water contact angle further decreased to 51°. The modification was characterized by IR (Fig. 3f), showing characteristic peaks of O–H stretching (3200-3500 cm^{-1}), C–H bending vibration (1342 cm^{-1}), S–H stretching (2585 cm^{-1}), the indole or indoline
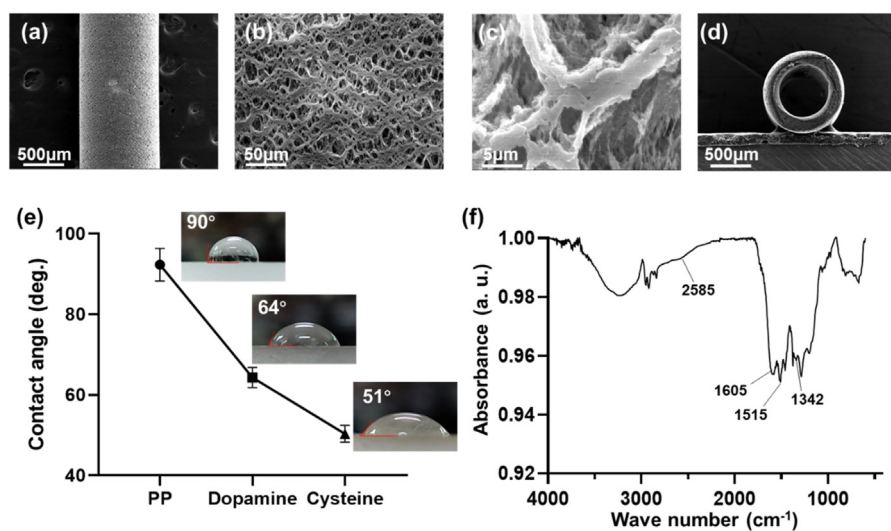

Fig. 3. SEM images of (a) untreated PP membrane, at a magnification of 50 × ; (b) untreated PP membrane, at a magnification of 500 × ; (c) untreated PP membrane, at a magnification of 5000 × ; and (d) Cross-sectional view of the prepared polypropylene membrane at a magnification of 50 × . The stainless-steel wire of the probe was removed in order to observe the detailed morphology. (e) Water contact angle for membrane M1, M2 and M3. (f) IR spectrum of polydopamine-cysteine coating.

structures and vibration of N–H (1515 cm^{-1} and 1605 cm^{-1}).

The efficiency of the microprobe for the sampling of lipids was demonstrated using the mouse brain sample. To ensure good reproductivity, the mouse brain tissue was homogenized and placed in a glass centrifuge tube for sampling by PPM microprobe. Lipids adsorbed on the microprobe was eluted with ACN/EtOAc/water (5/4/1, v/v/v), where PC 30:0 (10 µg/mL in eluent) was used as the internal standard (IS). As shown in Fig. 4, Table S1, Table S2 and Fig. S2, abundant peaks for several classes of lipids were detected, including phosphatidylcholine (PC), sphingomyelin (SM), phosphatidylethanolamine (PE), phosphatidylserine (PS), phosphatidylglycerol (PG), phosphatidylinositol (PI), and triacylglyceride (TAG). For comparison, the mouse brain homogenate was extracted by a most commonly used liquid-liquid extraction (LLE) method, the Folch method, which has high recovery for different classes of lipids, including glycerolipids, glycerophospholipids and sphingolipids (>75%) [41,42]. The relative abundances of PE, PS, PG, TAG and SM obtained from the PPM microprobe-based sampling was consistent with that obtained by the Folch method (Fig. 4c and Table S3). The relative abundance of PC obtained from the PPM microprobe-based sampling is slightly higher than the LLE method (100% vs 92.1%), while PI obtained from the PPM microprobe-based sampling is slightly lower than the LLE method (3.7% vs 4.1%). The number of different lipid subclasses in the eluates of LLE and PPM microprobes is shown in Fig. S3. These results showed the high recovery and wide coverage of the PPM microprobe for lipid sampling. It is worth noting that the sampling can be completed in 30 s in the analysis of lipids in the mouse brain tissues (Fig. S4a).

Solid material-based lipid extraction methods [43] are usually discriminative to different classes of lipids or different chain lengths within same class of lipids. For example, Giacometti et al. [44] reported a high recovery (~90%) for glycerolipids but a relatively low recovery (~60%) for polar lipids by an aminopropyl column. The PPM microprobe can make use of the feasibility of solid materials during sampling of tissue samples while showing comparable recoveries (76–110%) to the standard LLE methods [21–23]. The PPM microprobes were disposable, which could be conveniently prepared to a large number (~100) for further use in lipid sampling. The microprobes were also found to be stable when storing under room temperature for months. As shown in

Fig. S4b, the efficiency of the microprobes for the sampling of phospholipids from mouse brain tissues did not decrease obviously even after storage for 12 months.

3.2. Fast analysis of lipids in tissues based on the PPM microprobe and MS

As discussed above, the near-complete sampling of different classes of lipids from tissue samples can be achieved by simple sample preparaton steps. In this work, we also developed a workflow based on the PPM microprobe for the fast analysis of lipids from tissue samples. As shown in Fig. 5a, the workflow consists of three steps. In the sampling step, the microprobe was inserted into a tissue sample or rolled on the surface of a tissue sample for about 30 s. Since the sampling process did not require reaching extraction equilibrium of the lipids between each phase [45], the sampling can be completed in a short time. After sampling, a washing step was applied to remove pieces tissues or cells. This step can also remove salts from adsorbed lipids, which would be helpful to ionization of lipids by nanoESI. Relative quantitation was performed by calculating the intensity ratio of the target ion to the internal standard (PC 30:0, 10 ppm, I_{IS}). As can be seen in Fig. S4c, washing with water can significantly increase the intensity of the target phospholipid ions. Finally, the microprobe was inserted into a pulled glass tip filled with the elution solvent. By applying high voltages (~1500 V), desorption of lipids from the PPM and ionization of desorbed lipids would be realized. Conditions such as the washing solution type, washing time, elution solvent type and elution time were investigated and optimized. Through 3 sets of parallel experiments using mouse brain tissues, conditions were optimized to be: washing solution by water, and the elution solution was ACN/EtOAc/water 5/4/1 (v/v/v). Abundant peaks of lipids were obtained by nanoESI-MS (Fig. 5b), showing species of PC, PE, PS, PI, PG and SM. This workflow was also applied for fast profiling of lipids from other tissue samples such as mouse liver (Fig. 5c), leg (Fig. 5d) and stomach (Fig. 5e) tissues. Lipids obtained from the microprobe were also analyzed by the LC-MS method. In comparison with the nanoESI-MS method, LC-MS method can provide high sensitivity for the detection of some lipid subclasses such as PE (Fig. S5), since the ion suppression during ionization was reduced with chromatographic separation. It should be noted
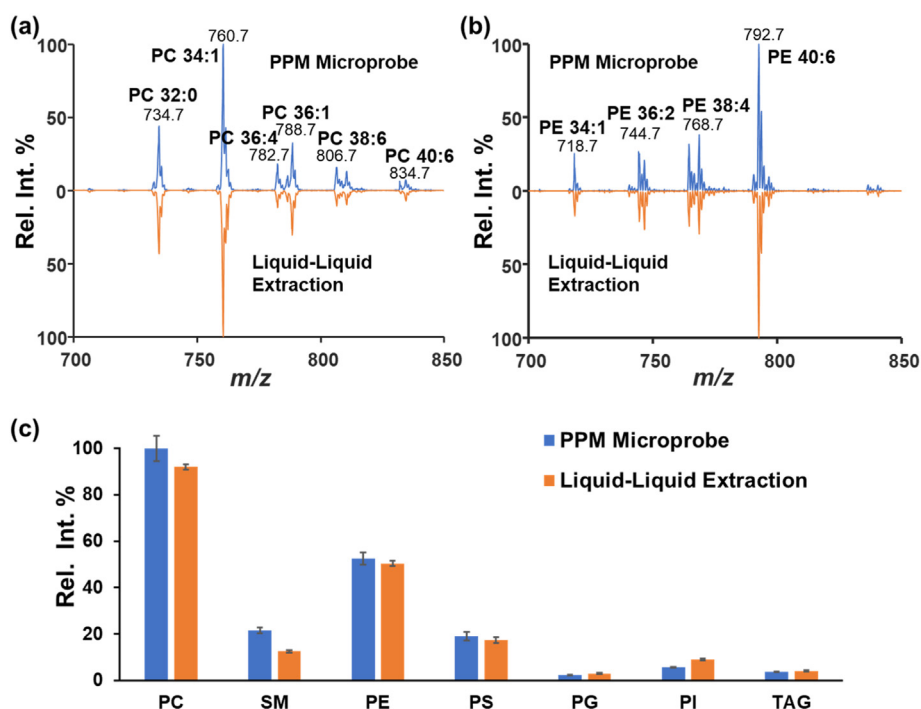

Fig. 4. Mass spectra of (a) PC and (b) PE in the mouse brain homogenate obtained by sampling with the PPM microprobe and liquid-liquid extraction. (c) Comparison of the extraction recoveries of different classes of lipid between the PPM sampling method and liquid-liquid extraction method (N = 3).
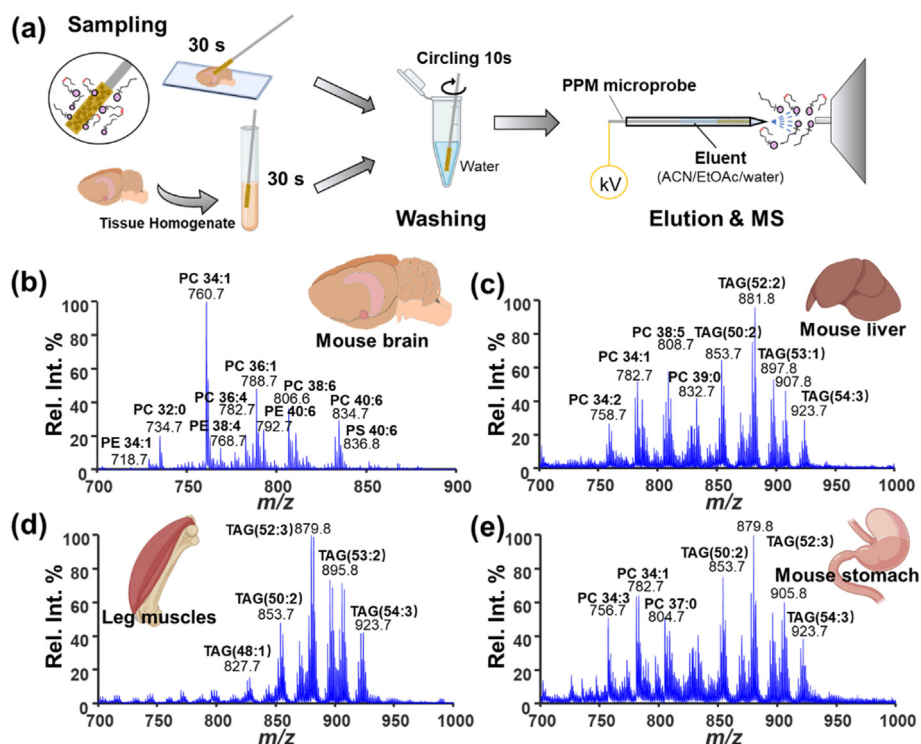
Fig. 5. (a) Steps of analysis of biological tissue by the PPM microprobe-based MS method. MS1 spectrum obtained by sampling of (b) mouse brain, (c) liver, (d) leg, and (e) stomach.

that the whole workflow of microsampling and nanoESI-MS took as less as 2 min, and did not require addition equipment for sample preparation, making it suitable to point-of-care applications.

Since the PPM has strong mechanical strength, it can be inserted into relative hard tissues for sampling of lipids at certain locations inside a tissue sample. This was demonstrated using a mouse kidney. As shown in Fig. 6a and b, lipids of the fibrous capsule of the mouse kidney was sampled by rolling the PPM probe on the surface for 30 s, while lipids from the renal medulla of the mouse kidney was sampled by inserting the PPM probe into the renal medulla (~3 mm under the fibrous capsule) and keeping for 30 s for sampling. From the characteristics of the spectral peaks in Fig. 6a and b, it can be seen that the lipid profiles have significant differences with the change of sampling depth. The content of TAG in the fibrous capsule is higher than that in the renal medulla (% abundance of 81.1% vs 41.8%), and the proportion of TAG with larger *m/z* is higher, while the internal PC and PE are more significant (percentage of total ion: 38.4% vs 11.4%). Some lipid species showed significant difference between the renal medulla and the fibrous capsule (Fig. 6c), such as PC 34:1, TAG 54:3, and TAG 54:4, with P values less than 0.001 (student's t-test). Results of sampling at different depths (surface, 1, 3, and 5 mm) were also obtained (Fig. S6), showing obvious depth-related variations in lipids such as PC 32:0, PC 38:4, and TAG 52:3.

3.3. Fast profiling of lipid C=C and sn-location isomers in tissue samples

The determination of the C=C position and its *sn*-position by MS enables the characterization of detailed structural moieties and the identification of lipid structural isomers. This has been partially realzied with the development of novel dissociation techniques such as ozone-induced dissociation [46], ultraviolet photodissociation [47], and derivatization-based tandem MS methods such as PB reaction [10]. With the development of LC-MS-based structural lipidomics platforms based on these methods, many lipid C=C and *sn*-location isomers have been revealed to be associated with diseases such as type 2 diabetes [48], breast cancer [9], thyroid cancer [49], medulloblastoma [50]. The PPM

microprobe could also be used for fast testing of potential lipid isomer biomarkers for biomedical applications.

A method was developed based on the procedure described in section 3.2 for fast identification of lipid C=C and *sn*-location isomers in tissue samples. After sampling by the PPM microprobe and washing, the microprobe was inserted into a glass capillary tip filled with solvent with PB reagent (2-acetylpyridine, 2-AP) (Fig. 7a). Applying UV light (254 nm, 6 W) onto the capillary tip, C=C of lipids in the solution can be derivatized by 2-AP, forming a four-ring structure, which can be cleaved under low-energy CID for identification of C=C locations (Fig. 7b). Using the sodium adduct of glycerophospholipid species, MS/MS can produce a dioxolane-type product, which can be further fragmented to product ions only containing the *sn*-1 chain information, allowing assignment of the *sn*-geometry (Fig. 7b). The capability of this method for fast analysis of lipid isomers was demonstrated by the mouse brain tissue. After sampling for 30 s and washing for 10 s, the PPM microprobe was inserted into 10 μL elution solution (ACN/EtOAc/water 5/4/1, with 20 mM 2-AP). Photochemical PB reaction was completed by applying UV light exposure for 30 s. Fig. 7c shows the example of PC 34:1 from the mouse brain tissue. After PB reaction, a product of [PBPC 34:1 + Na]+ (*m/z* 903.6 in positive ion mode) was obtained. MS/MS of this precursor ion produced a dioxolane-type product at *m/z* 720.6, which was further fragmented to obtain diagnostic product ions for C=C and *sn*-positions. PC 34:1 was identified to contain two *sn*-isomers of PC 16:0/18:1 (*m/z* 380.3 and *m/z* 396.2) and PC 18:1/16:0 (*m/z* 466.2), and the location of the C=C at C18:1 chain was identified to be *n9* (*m/z* 517.3 and *m/z* 606.5) and *n7* (*m/z* 489.2 and *m/z* 578.4). Other examples of lipid isomer identification in mouse brain tissue are shown in Fig. S7. These results showed that it was able to rapidly determine the lipid C=C and *sn*-isomers from tissue samples base on the PPM microprobe.

This method was also demonstrated for fast profiling of possible lipid isomer biomarkers from disease state tissue samples. Breast cancer is the most common and deadly cancer in women, and fortunately early screening can greatly improve patient survival rates [51]. Our previous study has revealed the differentiation of some phospholipid C=C isomers
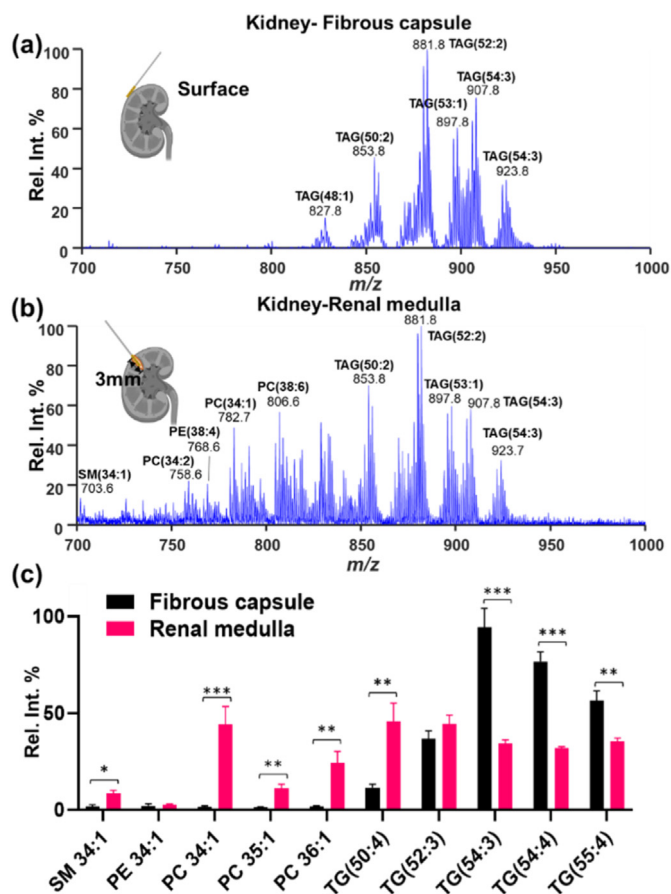
Fig. 6. The MS1 spectra sampled by the porous probe at the kidney (a) surface and at (b) a depth of 3 mm. (c) Comparison of relative abundance of lipid species from the renal medulla and the fibrous capsule. *P < 0.05, **P < 0.01, ***P < 0.001, Student's t-test.

between breast cancer and para-cancerous tissue samples [9]. In this work, a small-size breast cancer tissues (N = 3) and para-cancerous tissues (N = 3) were analyzed by the workflow described above. The ratio of isomer intensity was used for relative quantitation, which has been proven to be more sensitive in lipid biomarker discovery [9]. As shown in Fig. 7d, C=C of a series of phospholipids showed significant difference between cancerous and *para*-cacerous samples, such as the *n9/n7* ratios of PC 16:0_16:1, PC 16:0_18:1, PC 17:0_18:1 and PC 18:1_18:1. In addition, the MS1 spectra of two different types of tissues are shown in Fig. S8. These results showed that the PPM microprobe based workflow would be applicable for point-of-care determination of lipid isomer biomarkers for a wide range of biomedical applications.

3.4. Sampling of lipids from tissue samples by a microprobe array

Although small-scale sampling methods require less amount of tissues for testing and are less destructive to tissues, the heterogeneous distribution of molecules in the tissues may leading to significant variation of lipid profiles when sampling at different locations of a tissue. This has been demonstrated in many investigations of MS imaging of tissue samples [52]. In this work, we further designed a microprobe array for sampling of lipids at multiple sites simultaneously form a tissue sample. Fig. 8a shows an assay with 3 × 3 PPM microprobes. The diameter of the microprobe was 500 μm and the distance between the probe sampling points was 2 mm. Demonstrating on a whole mouse brain section, lipid information can be collected at 9 sites on the tissue separated by 2 mm. The sampling process of the assay is similar with that of the single microprobe. In a typical analysis, the microprobes of the assay were inserted into the tissue sample vertically, with the depth of ~2 mm (measured from the surface of the tissue to the end of the microprobe in the tissue). After sampling for 30 s, all the 9 microprobes would be adsorbed with lipids. After washing, each microprobe was inserted into the nanoESI tip for MS analysis sequentially. Using the microprobe assay, the reproducibility in the steps of tissue sampling, washing and elution could be improved. Due to the injection settings of the mass spectrometer, samples from different microprobes should be analyzed sequentially
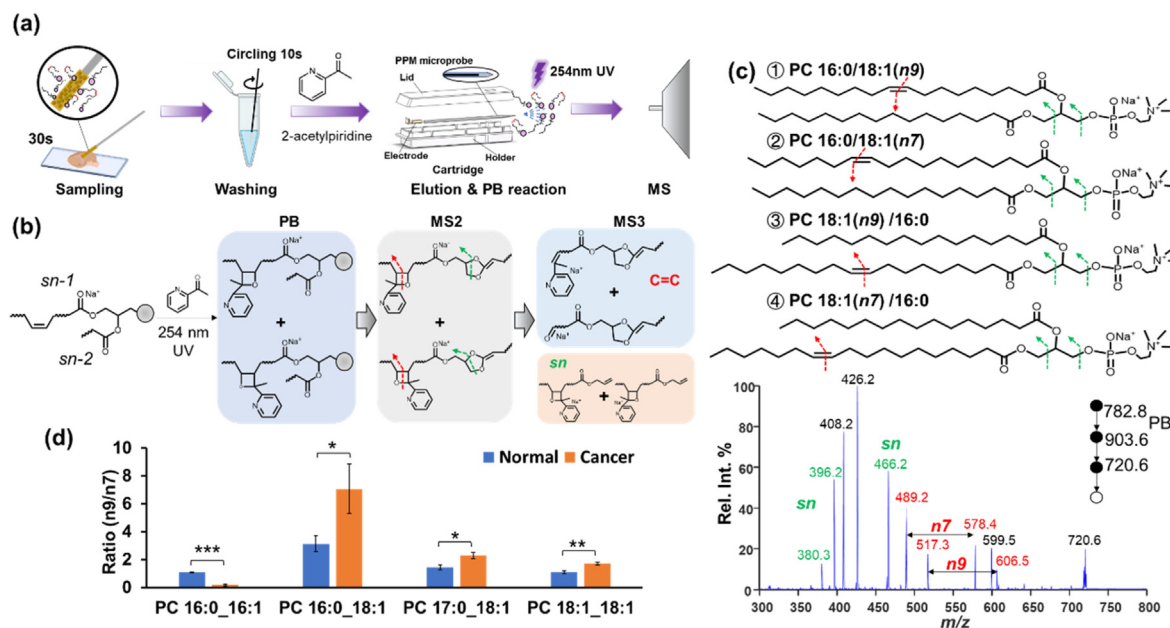

Fig. 7. (a) Process of sampling and MS analysis with PB reaction. (b) Mechanism of photochemical reaction between 2-AP and unsaturated phospholipids. (c) Mass spectrum for simultaneous identification of double bond and *sn*-positions of PC 34:1. (d) Relative isomer compositional analysis of C16:1 *n9/n7* and C18:1 *n9/n7* for PC in normal and cancerous breast tissue samples. *P < 0.05, **P < 0.01, ***P < 0.001, Student's t-test.
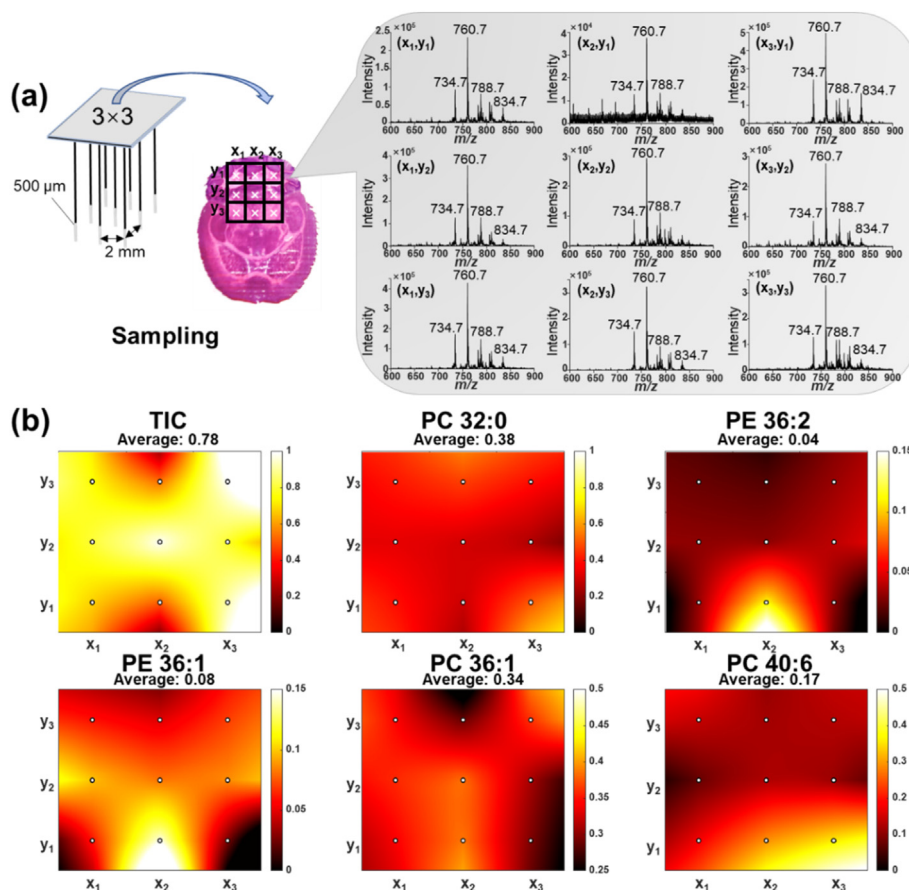
Fig. 8. (a) Schematic diagram of multi-point array sampling mass spectrometry analysis. (b) Ion images of TIC, PC 32:0, PE 36:2, PE 36:1, PC 36:1 and PC 40:6, all ion abundances are normalized to the strongest ion peak (PC 34:1) in the mass spectrum.

by MS. For the comparison of lipid species from different sites, the intensity of each PC was normalized with an endogenous phospholipid, which could improve the reproducibility of relative quantitation between different ionization processes. The data processing process was implemented on Matlab 2016b. As shown in Fig. 8b, obvious difference of lipid distribution was observed at 9 sample sites. Highly abundant PC 40:6 was detected at the (x_2, y_1) and (x_3, y_1) sites, while less PC 40:6 was detected on the (x_1, y_2) site. Through normalization to PC 34:1, ion images were drawn for the comparison of distribution of total lipids and commonly observed lipid species such as PC 32:0, PE 36:2, PE 36:1, PC 36:1 and PC 40:6. Significant differences were observed between different sites for the total ion intensities, with value variating from 0.52 to 1. The average intensity was calculated to be 0.78, which is consistent with the result obtained by sampling of the homogenate of a larger pieces of tissue section (Fig. S9). Similar results were obtained for the analysis of PC 32:0, PE 36:2, PE 36:1, PC 36:1 and PC 40:6 in the mouse tissue section. Besides providing average lipid information for the purpose of improving reproducibility of lipid profiling, the microprobe assay can also provide spatial distribution of lipid species rapidly, which can be useful for fast screening of special structures of tissue samples such as the border of cancerous tissues.

4. Conclusions

In this work, we developed a PPM microprobe for highly efficient sampling of lipids directly from tissue samples. The microprobe showed abundant micropores, good chemical resistance and high mechanical strength for direct sampling in different kinds of tissue samples. As a solid material, it also showed good feasibility during sampling while yielding high lipid recoveries (>76%) to different classes of lipids. A workflow was developed based on the microprobe for fast profiling of lipids in tissues by MS. Coupling with photochemical derivatization, the workflow also allowed for fast profiling of lipid C=C and sn-location isomers from tissue samples. The microprobe array can be used for simultaneous sampling at multiple sites, which could improve the sampling by small-scale tissue sampling methods. The PPM microprobe has the potential to be used for point-of-care lipid profiling and lipid isomer biomarker analysis in biomedical applications.

Credit author statement

W. Zhang and Z. Ouyang developed the idea and designed the experiments. B. Jiao, W. Zhou, and Y. Liu conducted the experiments and analyzed the data. B. Jiao and W. Zhang wrote the manuscript. W. Zhang and Z. Ouyang revised the manuscript. All authors have agreed to the published version of the manuscript.

Declaration of competing interest

The authors declare that they have no known competing financial interests or personal relationships that could have appeared to influence the work reported in this paper.

Data availability

Data will be made available on request.

Appendix A. Supplementary data

Supplementary data to this article can be found online at https://doi.org/10.1016/j.mtbio.2022.100424.

References

[1] P.L. Yèagle, Lipid regulation of cell membrane structure and function, FASEB J. 3 (1989) 1833–1842, https://doi.org/10.1096/fasebj.3.7.2469614.

[2] M. Cebecauer, M. Amaro, P. Jurkiewicz, M.J. Sarmento, R. Šachl, L. Cwiklik, M. Hof, Membrane lipid nanodomains, Chem. Rev. 118 (2018) 11259–11297, https://doi.org/10.1021/acs.chemrev.8b00322.

[3] S. Missaglia, R. Coleman, A. Mordente, D. Tavian, Neutral lipid storage diseases as cellular model to study lipid droplet function, Cells 8 (2019) 187, https://doi.org/10.3390/cells8020187.

[4] K. Simons, D. Toomre, Lipid rafts and signal transduction, Nat. Rev. Mol. Cell Biol. 1 (2000) 31–39, https://doi.org/10.1038/35036052.

[5] K.M. Eyster, The membrane and lipids as integral participants in signal transduction: lipid signal transduction for the non-lipid biochemist, Adv. Physiol. Educ. 31 (2007) 5–16, https://doi.org/10.1152/advan.00088.2006.

[6] M. Holzlechner, E. Eugenin, B. Prideaux, Mass spectrometry imaging to detect lipid biomarkers and disease signatures in cancer, Cancer Rep. 2 (2019), https://doi.org/10.1002/cnr2.1229.

[7] G. Zhao, H. Cardenas, D. Matei, Ovarian cancer—why lipids matter, Cancers 11 (2019) 1870, https://doi.org/10.3390/cancers11121870.

[8] G. von Minckwitz, M. Untch, J.-U. Blohmer, S.D. Costa, H. Eidtmann, P.A. Fasching, B. Gerber, W. Eiermann, J. Hilfrich, J. Huober, C. Jackisch, M. Kaufmann, G.E. Konecny, C. Denkert, V. Nekljudova, K. Mehta, S. Loibl, Definition and impact of pathologic complete response on prognosis after neoadjuvant chemotherapy in various intrinsic breast cancer subtypes, J. Clin. Orthod. 30 (2012) 1796–1804, https://doi.org/10.1200/JCO.2011.38.8595.

[9] W. Zhang, D. Zhang, Q. Chen, J. Wu, Z. Ouyang, Y. Xia, Online photochemical derivatization enables comprehensive mass spectrometric analysis of unsaturated phospholipid isomers, Nat. Commun. 10 (2019) 79, https://doi.org/10.1038/s41467-018-07963-8.

[10] W. Cao, S. Cheng, J. Yang, J. Feng, W. Zhang, Z. Li, Q. Chen, Y. Xia, Z. Ouyang, X. Ma, Large-scale lipid analysis with C=C location and sn-position isomer resolving power, Nat. Commun. 11 (2020) 375, https://doi.org/10.1038/s41467-019-14180-4.

[11] A. Villaseñor, J. Godzien, T.C. Barker-Tejeda, C. Gonzalez-Riano, Á. López-López, D. Dudzik, A. Gradillas, C. Barbas, Analytical approaches for studying oxygenated lipids in the search of potential biomarkers by LC-MS, TrAC - Trends Anal. Chem. 143 (2021), 116367, https://doi.org/10.1016/j.trac.2021.116367.

[12] A.S. Gandhi, D. Budac, T. Khayrullina, R. Staal, G. Chandrasena, Quantitative analysis of lipids: a higher-throughput LC–MS/MS-based method and its comparison to ELISA, Fut. Sci. OA 3 (2017) FSO157, https://doi.org/10.4155/fsoa-2016-0067.

[13] Y.S. Chhonker, S. Kanvinde, R. Ahmad, A.B. Singh, D. Oupický, D.J. Murry, Simultaneous quantitation of lipid biomarkers for inflammatory bowel disease using LC–MS/MS, Metabolites 11 (2021) 106, https://doi.org/10.3390/metabo11020106.

[14] T. Baba, J.L. Campbell, J.C.Y. Le Blanc, PaulR.S. Baker, K. Ikeda, Quantitative structural multiclass lipidomics using differential mobility: electron impact excitation of ions from organics (EIEIO) mass spectrometry, J. Lipid Res. 59 (2018) 910–919, https://doi.org/10.1194/jlr.D083261.

[15] M.C. Thomas, T.W. Mitchell, D.G. Harman, J.M. Deeley, J.R. Nealon, S.J. Blanksby, Ozone-induced dissociation: elucidation of double bond position within mass-selected lipid ions, Anal. Chem. 80 (2008) 303–311, https://doi.org/10.1021/ac7017684.

[16] D.D. Holden, J.S. Brodbelt, Improving performance metrics of ultraviolet photodissociation mass spectrometry by selective precursor ejection, Anal. Chem. 10 (2017), https://doi.org/10.1021/acs.analchem.6b03777.

[17] Y. Feng, B. Chen, Q. Yu, L. Li, Identification of double bond position isomers in unsaturated lipids by *m*-CPBA epoxidation and mass spectrometry fragmentation, Anal. Chem. 91 (2019) 1791–1795, https://doi.org/10.1021/acs.analchem.8b04905.

[18] H.-F. Li, W. Cao, X. Ma, X. Xie, Y. Xia, Z. Ouyang, Visible-light-driven [2 + 2] photocycloadditions between benzophenone and C=C bonds in unsaturated lipids, J. Am. Chem. Soc. 142 (2020) 3499–3505, https://doi.org/10.1021/jacs.9b12120.

[19] X. Zhao, W. Zhang, D. Zhang, X. Liu, W. Cao, Q. Chen, Z. Ouyang, Y. Xia, A lipidomic workflow capable of resolving *sn*- and C=C location isomers of phosphatidylcholines, Chem. Sci. 10 (2019) 10740–10748, https://doi.org/10.1039/C9SC03521D.

[20] X. Ma, W. Zhang, Z. Li, Y. Xia, Z. Ouyang, Enabling high structural specificity to lipidomics by coupling photochemical derivatization with tandem mass spectrometry, Acc. Chem. Res. 54 (2021) 3873–3882, https://doi.org/10.1021/acs.accounts.1c00419.

[21] J. Folch, M. Lees, G.H.S. Stanley, A simple method for the isolation and purification of total lipides from animal tissues, J. Biol. Chem. 226 (1957) 497–509, https://doi.org/10.1016/S0021-9258(18)64849-5.

[22] E.G. Bligh, W.J. Dyer, A rapid method of total lipid extraction and purification, Can. J. Biochem. Physiol. 37 (1959) 911–917, https://doi.org/10.1139/o59-099.

[23] P. Manirakiza, A. Covaci, P. Schepens, Comparative study on total lipid determination using Soxhlet, Roese-Gottlieb, Bligh & Dyer, and modified Bligh & Dyer extraction methods, J. Food Compos. Anal. 14 (2001) 93–100, https://doi.org/10.1006/jfca.2000.0972.

[24] A.P. Birjandi, F.S. Mirnaghi, B. Bojko, M. Wąsowicz, J. Pawliszyn, Application of solid phase microextraction for quantitation of polyunsaturated fatty acids in biological fluids, Anal. Chem. 86 (2014) 12022–12029, https://doi.org/10.1021/ac502627w.

[25] W. Zhang, S. Chiang, Z. Li, Q. Chen, Y. Xia, Z. Ouyang, A polymer coating transfer enrichment method for direct mass spectrometry analysis of lipids in biofluid samples, Angew. Chem. Int. Ed. 58 (2019) 6064–6069, https://doi.org/10.1002/anie.201900011.

[26] J. Deng, W. Li, Q. Yang, Y. Liu, L. Fang, Y. Guo, P. Guo, L. Lin, Y. Yang, T. Luan, Biocompatible surface-coated probe for *in vivo*, *in situ*, and microscale lipidomics of small biological organisms and cells using mass spectrometry, Anal. Chem. 90 (2018) 6936–6944, https://doi.org/10.1021/acs.analchem.8b01218.

[27] J. Deng, Y. Yang, Y. Liu, L. Fang, L. Lin, T. Luan, Coupling paternò-büchi reaction with surface-coated probe nanoelectrospray ionization mass spectrometry for in vivo and microscale profiling of lipid C=C location isomers in complex biological tissues, Anal. Chem. 91 (2019) 4592–4599, https://doi.org/10.1021/acs.analchem.8b05803.

[28] Y. Lv, X. Yu, J. Jia, S.-T. Tu, J. Yan, E. Dahlquist, Fabrication and characterization of superhydrophobic polypropylene hollow fiber membranes for carbon dioxide absorption, Appl. Energy 90 (2012) 167–174, https://doi.org/10.1016/j.apenergy.2010.12.038.

[29] J.A. Franco, S.E. Kentish, J.M. Perera, G.W. Stevens, Fabrication of a superhydrophobic polypropylene membrane by deposition of a porous crystalline polypropylene coating, J. Membr. Sci. 318 (2008) 107–113, https://doi.org/10.1016/j.memsci.2008.02.032.

[30] B. Zhou, Y. Tang, Q. Li, Y. Lin, M. Yu, Y. Xiong, X. Wang, Preparation of polypropylene microfiltration membranes via thermally induced (solid-liquid or liquid-liquid) phase separation method, J. Appl. Polym. Sci. 132 (2015) 42490, https://doi.org/10.1002/app.42490.

[31] Y. Ren, J. Liu, L. Li, M.N. McLuckey, Z. Ouyang, Direct mass spectrometry analysis of untreated samples of ultralow amounts using extraction nano-electrospray, Anal. Methods 5 (2013) 6686, https://doi.org/10.1039/c3ay41149d.

[32] H. Wang, J. Liu, R.G. Cooks, Z. Ouyang, Paper spray for direct analysis of complex mixtures using mass spectrometry, Angew. Chem. Int. Ed. 49 (2010) 877–880, https://doi.org/10.1002/anie.200906314.

[33] Y. Ren, S. Chiang, W. Zhang, X. Wang, Z. Lin, Z. Ouyang, Paper-capillary spray for direct mass spectrometry analysis of biofluid samples, Anal. Bioanal. Chem. 408 (2016) 1385–1390, https://doi.org/10.1007/s00216-015-9129-9.

[34] Z. Takats, J.M. Wiseman, B. Gologan, G.R. Cooks, Mass spectrometry sampling under ambient conditions with desorption electrospray ionization, Science 306 (2004) 471–473, https://doi.org/10.1126/science.1104404.

[35] L.S. Eberlin, I. Norton, D. Orringer, I.F. Dunn, X. Liu, J.L. Ide, A.K. Jarmusch, K.L. Ligon, F.A. Jolesz, A.J. Golby, S. Santagata, N.Y.R. Agar, R.G. Cooks, Ambient mass spectrometry for the intraoperative molecular diagnosis of human brain tumors, Proc. Natl. Acad. Sci. USA 110 (2013) 1611–1616, https://doi.org/10.1073/pnas.1215687110.

[36] J.D. Harper, N.A. Charipar, C.C. Mulligan, X. Zhang, R.G. Cooks, Z. Ouyang, Low-temperature plasma probe for ambient desorption ionization, Anal. Chem. 80 (2008) 9097–9104, https://doi.org/10.1021/ac801641a.

[37] K.-C. Schäfer, J. Dønes, K. Albrecht, T. Szaniszló, J. Balog, Rø Skoumal, M. Katona, M. Tóth, L. Balogh, Z. Takµts, In vivo, in situ tissue analysis using rapid evaporative ionization mass spectrometry, Angew. Chem. Int. Ed. 3 (2009), https://doi.org/10.1002/anie.200902546.

[38] H. Lee, S.M. Dellatore, W.M. Miller, P.B. Messersmith, Mussel-inspired surface chemistry for multifunctional coatings, Science 318 (2007) 426–430, https://doi.org/10.1126/science.1147241.

[39] P. Li, X. Cai, D. Wang, S. Chen, J. Yuan, L. Li, J. Shen, Hemocompatibility and anti-biofouling property improvement of poly(ethylene terephthalate) via self-polymerization of dopamine and covalent graft of zwitterionic cysteine, Colloids Surf. B Biointerfaces 110 (2013) 327–332, https://doi.org/10.1016/j.colsurfb.2013.04.044.

[40] R. Shevate, M. Kumar, M. Karunakaran, M.N. Hedhili, K.-V. Peinemann, Polydopamine/Cysteine surface modified isoporous membranes with self-cleaning properties, J. Membr. Sci. 529 (2017) 185–194, https://doi.org/10.1016/j.memsci.2017.01.058.

[41] K. Yang, X. Han, Lipidomics: techniques, applications, and outcomes related to biomedical Sciences, Trends Biochem. Sci. 41 (2016) 954–969, https://doi.org/10.1016/j.tibs.2016.08.010.

[42] B. Reichl, N. Eichelberg, M. Freytag, J. Gojo, A. Peyrl, W. Buchberger, Evaluation and optimization of common lipid extraction methods in cerebrospinal fluid samples, J. Chromatogr. B 1153 (2020), 122271, https://doi.org/10.1016/j.jchromb.2020.122271.

[43] B. Bojko, K. Gorynski, G.A. Gomez-Rios, J.M. Knaak, T. Machuca, V.N. Spetzler, E. Cudjoe, M. Hsin, M. Cypel, M. Selzner, M. Liu, S. Keshavjee, J. Pawliszyn, Solid phase microextraction fills the gap in tissue sampling protocols, Anal. Chim. Acta 803 (2013) 75–81, https://doi.org/10.1016/j.aca.2013.08.031.

[44] J. Giacometti, A. Milošević, C. Milin, Gas chromatographic determination of fatty acids contained in different lipid classes after their separation by solid-phase extraction, J. Chromatogr. A 976 (2002) 47–54, https://doi.org/10.1016/S0021-9673(02)01159-7.

[45] D.S. Kulyk, T. Sahraeian, S. Lee, A.K. Badu-Tawiah, Microsampling with a solid-phase extraction cartridge: storage and online mass spectrometry analysis, Anal. Chem. 93 (2021) 13632–13640, https://doi.org/10.1021/acs.analchem.1c02960.

[46] D.L. Marshall, H.T. Pham, M. Bhujel, J.S.R. Chin, J.Y. Yew, K. Mori, T.W. Mitchell, S.J. Blanksby, Sequential collision- and ozone-induced dissociation enables assignment of relative acyl chain position in triacylglycerols, Anal. Chem. 88 (2016) 2685–2692, https://doi.org/10.1021/acs.analchem.5b04001.

[47] J.S. Brodbelt, L.J. Morrison, Ultraviolet photodissociation mass spectrometry for analysis of biological molecules, Chem. Rev. 120 (2019) 53, https://doi.org/10.1021/acs.chemrev.9b00440.

[48] S. Becher, P. Esch, S. Heiles, Relative quantification of phosphatidylcholine *sn*-isomers using positive doubly charged lipid–metal ion complexes, Anal. Chem. 90 (2018) 11486–11494, https://doi.org/10.1021/acs.analchem.8b02731.

[49] J. Zhang, X. Huo, C. Guo, X. Ma, H. Huang, J. He, X. Wang, F. Tang, Rapid imaging of unsaturated lipids at an isomeric level achieved by controllable oxidation, Anal. Chem. 93 (2021) 2114–2124, https://doi.org/10.1021/acs.analchem.0c03888.

[50] M.R.L. Paine, B.L.J. Poad, G.B. Eijkel, D.L. Marshall, S.J. Blanksby, R.M.A. Heeren, S.R. Ellis, Mass spectrometry imaging with isomeric resolution enabled by ozone-induced dissociation, Angew. Chem. Int. Ed. 57 (2018) 10530–10534, https://doi.org/10.1002/anie.201802937.

[51] Z. Momenimovahed, H. Salehiniya, Epidemiological characteristics of and risk factors for breast cancer in the world, Breast Cancer 11 (2019) 151–164, https://doi.org/10.2147/BCTT.S176070.

[52] D. Zhou, S. Guo, M. Zhang, Y. Liu, T. Chen, Z. Li, Mass spectrometry imaging of small molecules in biological tissues using graphene oxide as a matrix, Anal. Chim. Acta 962 (2017) 52–59, https://doi.org/10.1016/j.aca.2017.01.043.